

spots is comparable to that observed for an ordinary nuclear reflection. (b) The spots in the neighborhood of each reciprocal lattice point exhibit octahedral spatial symmetry with relative intensities as shown in the figure. (c) The separation of the spots along the axes of each octahedron is $1/39 \text{ \AA}^{-1}$.

The following model accounts for the above observations. The antiferromagnetic structure of chromium (bcc) is one in which the body-centered spin is antiparallel to the corner spin. The splitting of the superstructure peaks is produced by platelike antiphase domains in which 180° spin reversals in the antiferromagnetic spin arrangement occur every 14 unit cells normal to the antiphase boundaries as follows:

+ - - - - - - - - - - { - - - - - - - - - - } + - - - etc.

These antiphase domain boundaries are parallel to the crystallographic cube faces, but the crystal as a whole consists of a random arrangement of regions in any one of which the domain boundary is parallel to a particular cube face. Within a domain the spins are parallel to the domain boundary. It is this restriction on spin direction which accounts for the observed relative intensities of the spots in the reciprocal lattice given in Fig. 2 since the magnetic intensity depends on the relative orientations of the spin and scattering vectors.

From the integrated intensities of the magnetic superstructure peaks (100), (111), and (210), the Bohr magneton number is found to be 0.4 ± 0.05 in agreement with Shull and Wilkinson.³ It was also

found that the magnetic form factor is in agreement with that of Mn^{2+} .⁴ The magnetic intensity of the (100) peak as a function of temperature agreed with that derived from the Brillouin function for spin $\frac{1}{2}$ and gave a Néel temperature of $35^\circ\text{C} \pm 2^\circ$ which coincides with other physical anomalies such as resistivity, Young's modulus, and lattice expansion. This temperature, however, is not in agreement with powder neutron diffraction data previously reported by Shull and Wilkinson³ ($T_N \cong 175^\circ\text{C}$) and recently confirmed by us.

The origin of the antiphase domains is not known but a recent proposal of Kaplan⁵ points out the possibility of lowering the energy by virtue of a nearest and next-nearest neighbor interaction, both of which are antiferromagnetic. In his proposed model the spins do not make an abrupt 180° reversal but rather spiral with a fixed period.

We wish to thank Professor C. G. Shull for his help in the initial experiments, Dr. T. Kaplan for discussions, and Dr. Earl Hays of the Bureau of Mines for supplying us with several samples of chromium.

* Research performed under the auspices of the U. S. Atomic Energy Commission.

¹These crystals were supplied by Dr. H. Lipsitt at Wright Air Development Center.

²C. H. Johansson and J. O. Linde, *Ann. Physik* **25**, 1 (1936).

³C. G. Shull and M. K. Wilkinson, *Revs. Modern Phys.* **25**, 100 (1953).

⁴Corliss, Elliott, and Hastings, *Phys. Rev.* **104**, 924 (1956).

⁵T. Kaplan (private communication).

HYPERFINE COUPLING IN CoFe AND CoNi ALLOYS AS DETERMINED BY HEAT CAPACITY MEASUREMENTS*

V. Arp,† D. Edmonds, and R. Petersen

Department of Physics, University of California, Berkeley, California

(Received August 5, 1959)

Each nucleus in a ferromagnet experiences an effective magnetic field (H_{eff}) caused by the hyperfine interaction with unpaired electrons. Marshall¹ has calculated the various contributions to this effective field and has shown how these contributions may be expected to depend on the electronic configuration surrounding the nucleus. The hyperfine interaction gives rise to a nuclear polarization at low temperatures and to a nuclear contribution to the specific heat

given by

$$\frac{C}{Nk} = \frac{1}{3} \frac{I+1}{I} \left(\frac{\mu H_{\text{eff}}}{kT} \right)^2 + O \left(\frac{\mu H_{\text{eff}}}{kT} \right)^4,$$

where N is the number of nuclei, μ and I are the nuclear moment and spin, respectively, and k is Boltzmann's constant. Similar contributions to the specific heat in a ferromagnetic metal have previously been measured in cobalt²⁻⁴ and

terbium.^{4,5}

We have measured the specific heat of some CoFe and CoNi alloys in order to obtain further information about the electronic configuration in these iron group elements in connection with the suggestion of Weiss⁶ that only about two 3*d* electrons are localized around each iron atom in metallic iron, whereas the conventional numbers of 3*d* electrons are 8.3 and 9.4 for metallic cobalt and nickel, respectively. The naturally occurring isotopes of iron and nickel have zero nuclear magnetic moment, whereas that of cobalt (Co⁵⁹) has a nuclear moment of 4.583 nuclear magnetons and a spin of 7/2. Thus the nuclear specific heat measured in the CoFe and CoNi alloys enables one to deduce the value of H_{eff} acting at a cobalt nucleus.

An annealed sample of alloy weighing about 12 grams was suspended inside a standard demagnetizing cryostat and linked through a lead superconducting thermal switch to a paramagnetic salt. By adiabatic demagnetization of the salt the sample was cooled to 0.35°K and then thermally isolated from the salt. The temperature of the sample was measured by means of a carbon resistance thermometer which was calibrated from 1°K to 0.35°K against the measured susceptibility of the paramagnetic salt during each experiment. Specific heat measurements were made in the range 0.35°K to 0.7°K. In this range only the nuclear ($\propto T^{-2}$) and electronic ($\propto T$) contributions to the specific heat are appreciable; the total specific heat has the form $C = aT^{-2} + bT$. By plotting CT^2 against T^3 a straight line was obtained from which the separate contributions were directly obtained. The experimental results are shown in Table I. The electronic specific heats of cobalt and iron are in reasonable agreement with the previously measured value

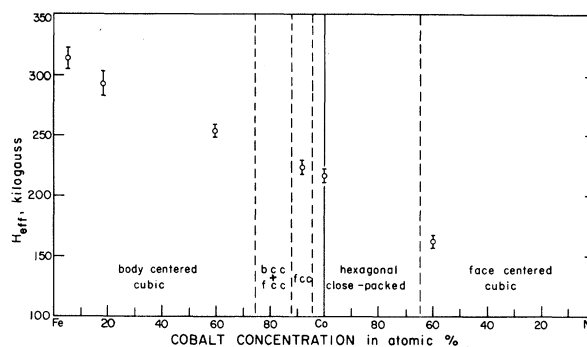


FIG. 1. Values of the effective (hyperfine) field as a function of cobalt concentration.

of 5.0T millijoules/mole °K for both cobalt and iron.⁷ In Fig. 1 the values of H_{eff} are plotted against cobalt concentration. The crystal structure of each specimen indicated in Fig. 1 was checked by x-ray diffraction of the specimen.

The approximately linear relation obtained in Fig. 1 gives no hint of any discontinuities in H_{eff} such as might be expected if the electronic configuration around each iron atom, and hence around each cobalt atom, were to change rapidly in a narrow concentration range. Such a rapid change, coming from an increase in the number of 3*d* electrons localized at each iron atom, has been postulated by Lomer and Marshall⁸ to occur at about 35% Co in Fe, and by Mott and Stevens⁹ at the bcc-fcc phase transition. Furthermore in the alloys of cubic structure the dipolar contribution to H_{eff} is zero, while in hexagonal cobalt the dipolar contribution has been estimated by Marshall to be some 81 kilogauss. There are however theoretical reasons to believe that this figure was considerably overestimated, as the band character was neglected entirely in making the estimate. Figure 1 shows that H_{eff} in hexag-

Table I. Experimental results.

| Alloy
[atomic %] | Specific heat
[millijoules (mole °K) ⁻¹] | H_{eff}
[kilogauss] |
|---------------------|---|---------------------------------|
| 60.0 Co, 40.0 Ni | $(1.55 \pm 0.07)(1/T^2) + (7.5 \pm 0.4)T$ | 161 ± 3 |
| 100 Co | $(4.78 \pm 0.12)(1/T^2) + (5.6 \pm 0.3)T$ | 219 ± 4 |
| 91.5 Co, 8.5 Fe | $(4.56 \pm 0.12)(1/T^2) + (4.7 \pm 0.7)T$ | 223 ± 4 |
| 58.7 Co, 41.3 Fe | $(3.87 \pm 0.07)(1/T^2) + (4.3 \pm 0.2)T$ | 256 ± 3 |
| 17.2 Co, 82.8 Fe | $(1.48 \pm 0.10)(1/T^2) + (3.8 \pm 0.3)T$ | 293 ± 10 |
| 4.8 Co, 95.2 Fe | $(0.47 \pm 0.03)(1/T^2) + (4.7 \pm 0.2)T$ | 314 ± 9 |
| 100 Fe | $(0.1 \pm 0.2)(1/T^2) + (4.9 \pm 0.5)T$ | ... |

onal cobalt has essentially the value one would deduce from the approximately linear variation found in the cubic alloys.

Our thanks are due to Dr. N. Kurti for his initial stimulus in this investigation, to Dr. C. Kittel for his continued interest, and to Dr. W. Marshall for many discussions.

*Supported by the National Science Foundation.

[†]Now at the National Bureau of Standards, Boulder, Colorado.

¹W. Marshall, Phys. Rev. **110**, 1280 (1958).

²C. V. Herr and R. A. Erickson, Phys. Rev. **108**, 896 (1957).

³Arp, Kurti, and Petersen, Bull. Am. Phys. Soc. **2**, 388 (1957).

⁴N. Kurti, Suppl. J. Appl. Phys. **30**, 215 (1959).

⁵N. Kurti and R. S. Safrata, Phil. Mag. **3**, 780 (1958).

⁶W. Marshall and R. J. Weiss, Suppl. J. Appl. Phys. **30**, 220 (1959).

⁷P. H. Keesom and N. Pearlman, *Handbuch der Physik*, edited by S. Flügge (Springer-Verlag, Berlin, 1956), Vol. 14, p. 322.

⁸W. Lomer and W. Marshall, Phil. Mag. **3**, 185 (1958).

⁹N. F. Mott and K. W. Stevens, Phil. Mag. **2**, 1364 (1957).

ELECTROLUMINESCENCE AT POINT CONTACTS IN CUPROUS OXIDE AND THE MOBILITY OF Cu^+ IONS AT ROOM TEMPERATURE

R. Frerichs and I. Liberman

Department of Electrical Engineering, Northwestern University, Evanston, Illinois

(Received August 3, 1959)

The observation of electroluminescence in Cu_2O between -50 and $+50^\circ\text{C}$ ¹ makes it possible to study the very small mobility of Cu^+ ions in this temperature range. Cu^+ vacancies, which are involved in the radiation emission in Cu_2O , are moved from the cathode, where the emission takes place, to the anode by the same field which produces the electroluminescence. In a one-dimensional arrangement this effect can be used to study the mobility of Cu^+ vacancies, which is of course identical with that of the Cu^+ ions.

A flattened copper wire ($d=0.5$ mm) is oxidized at 1040°C , cooled in high vacuum, and mounted with four electrodes in a glass vacuum container (Fig. 1). A field of 800 volts/cm which moves

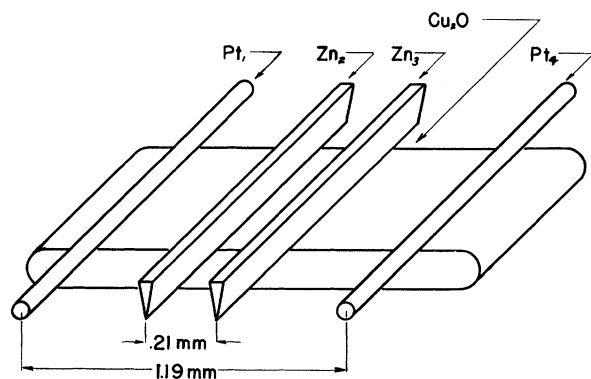


FIG. 1. Arrangement of electrodes on cuprous oxide.

the vacancies is applied between two platinum electrodes, Pt_1 and Pt_4 , which are spaced 1.2 mm apart and are pressed by springs onto the Cu_2O . Platinum, due to its high work function, forms ohmic contacts with the p -type Cu_2O . The electroluminescence is observed at two zinc knife edges, Zn_2 and Zn_3 , which are spaced 0.21 mm apart. Zinc with its low work function forms rectifying contacts with Cu_2O . A barrier layer at the cathode is the necessary condition for the generation of electroluminescence in this material. The radiation pulses ($\lambda=0.8$ to 1.2μ) are studied with an infrared-sensitive photomultiplier, a double-trace cathode-ray oscilloscope, and a Polaroid camera. Alternate periods of "driving" the vacancies by the dc field applied to Pt_1 and Pt_4 and of "reading out" the concentration of the vacancies at the electrodes Zn_2 and Zn_3 with ac (200 cycles/sec, 60 volts) are used (Fig. 2). If the distribution of the vacancies at the beginning of the experiment is uniform throughout the sample, a field in the direction $\text{Pt}_4 \rightarrow \text{Pt}_1$ will drive them towards Pt_4 . The radiation pulses at Zn_2 and Zn_3 are observed at the scope. As the "read-out" voltage is simultaneously shown at the second trace of the scope, the radiation pulses which show up at the negative electrode can be coordinated to Zn_2 or Zn_3 . The "read-out" period is short (2 sec) in order to prevent additional motion of the vacancies due to the ac field.

Figure 2 gives the radiation pulses as function